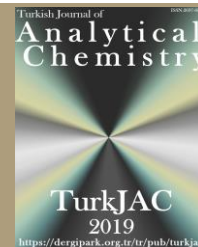




TurkJAC

Turkish Journal of

## Analytical Chemistry

<https://dergipark.org.tr/tr/pub/turkjac>
TurkJAC  
2019
<https://dergipark.org.tr/tr/pub/turkjac>

## Synthesis and characterization of biocopolymer kappa-Carrageenan( $\kappa$ -C)-g-polyacrylamide/activated bentonite composite\*

Kamel Ismet Benabadji<sup>1\*\*</sup> , Tayeb Hocine<sup>1</sup> , Oussama Bouras<sup>1</sup> , Bouras Brahim<sup>1</sup> ,  
Noussaiba Kheir<sup>1</sup>

<sup>1</sup> University of Tlemcen, Faculty of Sciences, Department of Chemistry, Laboratory of Organic Electrolyte and Polyelectrolytes Application (LAEPO), BP 119, 13000, Tlemcen, Algeria

### Abstract

In the last decade, there is an increased interest to use biodegradable materials. In the present study, new composites based on activated bentonite (BNA)/kappa-Carrageenan ( $\kappa$ -C)/acrylamide (AM) have been prepared by graft copolymerization of AM and kappa-Carrageenan ( $\kappa$ -C) in the presence of activated bentonite (BNA) clay powder, and ammonium persulfate (APS) as an initiator. Different component concentrations of AM and  $\kappa$ -C were used by maintaining 1 g of BNA in all types of composites.

We focused on the interactions between mineral clay structure and polymer matrices.

The structure and morphology of these materials were investigated by FT-IR and XRD, while the thermal properties were tested using TGA.

Evidence of grafting and BNA interaction was obtained by comparison of FTIR and TGA spectra of the initial substrates and the composites. The apparition of new absorption bands at 1256 cm<sup>-1</sup>, 922 cm<sup>-1</sup>, and 843 cm<sup>-1</sup> confirmed the presence of sulfate groups and correspond to the sulfonic acid group, C-O stretching band, 3, 6-anhydro-D-galactose and glycosidic linkages of  $\kappa$ -C backbone, in the composite structure. Electrostatic interactions and/or hydrogen bonds may have occurred between BNA and ( $\kappa$ -C/AM) copolymer.

TGA analysis showed the thermal stability improved by adding BNA clay particles.

The formation of intercalated nanocomposites in the case of C1 ((BNA/ $\kappa$ -C/AM) (1/0.5/0.5)), C2 ((BNA/ $\kappa$ -C/AM) (1/1/0.5)), C3 ((BNA/ $\kappa$ -C/AM) (1/0.5/1)) and C4((BNA/ $\kappa$ -C/AM) (1/1/1)) samples was confirmed by XRD analysis. The shift of peak attributed to montmorillonite in the several composites except C4 to lower angles in XRD diffractometer suggests the formation of intercalated nanocomposites.

The absence of the basal peak corresponding to montmorillonite phase in the case of C4 composite suggests a high dispersion of clay platelets, named exfoliation in the nanocomposite material.

The obtained results from this study suggest that the prepared composites could be effectively applied for removing cationic dyes from aqueous solutions.

**Keywords:** Acrylamide, activated bentonite, carrageenan, composite

### 1. Introduction

The treatment of contaminated wastewater is one of the most serious environmental problems faced by chemical, pharmaceutical, textile, polymer, plastic, and leather industries. Recently, much attention has been focused on the use of a new generation of absorbent composites. These materials are essentially prepared by including inorganic clays into the polymeric matrix.

Due to their large surface area and high cation exchange capacity, clays such as montmorillonite [1,2] and bentonite [3], have been studied for potential applications as environmental remediation adsorbent

for heavy metals and organic compounds adsorption. The addition of these types of minerals in a composite mixture not only improves some properties such as swelling ability, gel strength, mechanical, and thermal stability but also significantly reduces production cost [4–6]. However, for extensive process utilization, most of these materials are not suitable. To resolve these issues, modification of conventional adsorbents by using a polysaccharide matrix is an ideal alternative.

Among the most abundant polysaccharides, carrageenans are soluble polysaccharides extracted from

**Citation:** K.I. Benabadji, T. Hocine, O. Bouras, B. Brahim, N. Kheir, Synthesis and characterization of biocopolymer kappa-Carrageenan( $\kappa$ -C)-g-polyacrylamide/activated bentonite composite, Turk J Anal Chem, 7(2), 2025, 79–84.

**\*\*Author of correspondence:** [bismetdz@yahoo.fr](mailto:bismetdz@yahoo.fr)

**Tel:** +00213771872929

**Fax:** N/A

**Received:** December 30, 2024 **Accepted:** March 14, 2025

**doi** <https://doi.org/10.51435/turkjac.1610186>

\*This paper was presented at the 6th International Environmental Chemistry Congress, EnviroChem 05-08 November 2024, Trabzon Türkiye.

red seaweeds. They have strong gel-forming ability and are biocompatible. They consist of long linear chains of D-anhydrogalactose and D-galactose with anionic sulfate groups ( $-\text{OSO}_3^-$ ) [7]. There are three types of carrageenans: kappa ( $\kappa$ ), iota ( $\iota$ ), and lambda ( $\lambda$ ) which differ in sulfate ester and 3,6-anhydro- $\alpha$ -D-galactopyranosyl content. Their water solubility is strongly related to the content of sulfate groups and associated ions.

The structure of  $\kappa$ -carrageenan consists of the 4-sulfate-O- $\beta$ -D-galactopyranosyl-(1,4)-3,6-anhydro- $\alpha$ -D-galactose units [8]. It is commonly used as a thickening and stabilizing agent in prepared foods, cosmetics, and pharmaceuticals.  $\kappa$ -Carrageenan has also been used to prepare biodegradable films for biomedical applications [9].

Due to their high biodegradability, biocompatibility, and nontoxicity, hydrogels based on carrageenans have been also used as potential adsorbents for eliminating pollution like dyes from aqueous solutions [10,11].

Moreover, the combination of diverse structures like bentonite nanoclay [12], montmorillonite clay [13] and other nanomaterials with carrageenan has paved the way for scientists to prepare new materials with interesting properties.

Including inorganic clays into a polymeric matrix improves some properties of plastics and gels [14]. A new generation of adsorbent composites was prepared by incorporating montmorillonite [15], attapulgite [16–18], kaolin [19–21], hydrotalcite [22,23], mica [24], bentonite [25,26] and laponite [27] into polymeric matrices. OH reactive groups contained on layered aluminosilicate surface are enabled to interact with reactive sites of natural polymers and monomers and lead to the formation of composites with high adsorption capacities.

The aim of this study was to develop new composites based on  $\kappa$ -carrageenan, acrylamide and activated bentonite.

## 2. Experimental

### 2.1. Materials and methods

Acrylamide (AM), ammonium persulfate [APS], and kappa-Carrageenan ( $\kappa$ -C) were supplied by Merck. In our earlier work, we prepared activated bentonite (BNA) by modifying raw clay (RC) particles [28]. The solid phase of RC was dispersed in a sodium chloride solution (1M). This operation was repeated three times. To remove excess salt, the resulting solid after saturation was washed with bidistilled water several times; the final product was BNA. The hexamminecobalt(III) chloride was used to determine the cation exchange capacity (CEC), which was found to be equal to 85 meq/g/100 g.

A series of BNA/ $\kappa$ -C/AM with different contents of  $\kappa$ -C and AM was simply prepared. A constant mass weight of BNA was used (Table 1).

The  $\kappa$ -C solution has been prepared by slow addition of a weighted amount of  $\kappa$ -C powder to bidistilled water in a 100-mL three-necked flask equipped with a mechanical stirrer and a reflux condenser. The solution was heated to 65 °C. After complete dissolution of  $\kappa$ -C, APS initiator (0.1 g dissolved in 3 mL distilled water) was added and kept at 65 °C for 10 min to generate radicals. 1 g of BNA particles was dispersed separately in 12 mL of distilled water and 5 mL of monomer solution containing pre-weighted amount of AM was added. This mixture was poured into the flask containing  $\kappa$ -C radicals. The temperature was raised to 80 °C and maintained for 1 hour to complete the reaction.

After 24 hours, the obtained composite was precipitated by pouring it into the water/absolute ethanol mixture (ratio 1:5). The precipitate was filtered and subsequently dried in an oven at 75 °C for 24 hours.

The codes and the composition of composites are presented in Table 1.

**Table 1.** Sample codes and composition

Code	$\kappa$ -Carrageenan mass (g)	Acrylamide mass (g)	BNA mass (g)
C1 (BNA/ $\kappa$ -C/AM) (1/0.5/0.5)	0.5	0.5	1
C2 (BNA/ $\kappa$ -C/AM) (1/1/0.5)	1	0.5	1
C3 (BNA/ $\kappa$ -C/AM) (1/0.5/1)	0.5	1	1
C4 (BNA/ $\kappa$ -C/AM) (1/1/1)	1	1	1

#### 2.1.1. Fourier transform infrared spectroscopy (FTIR)

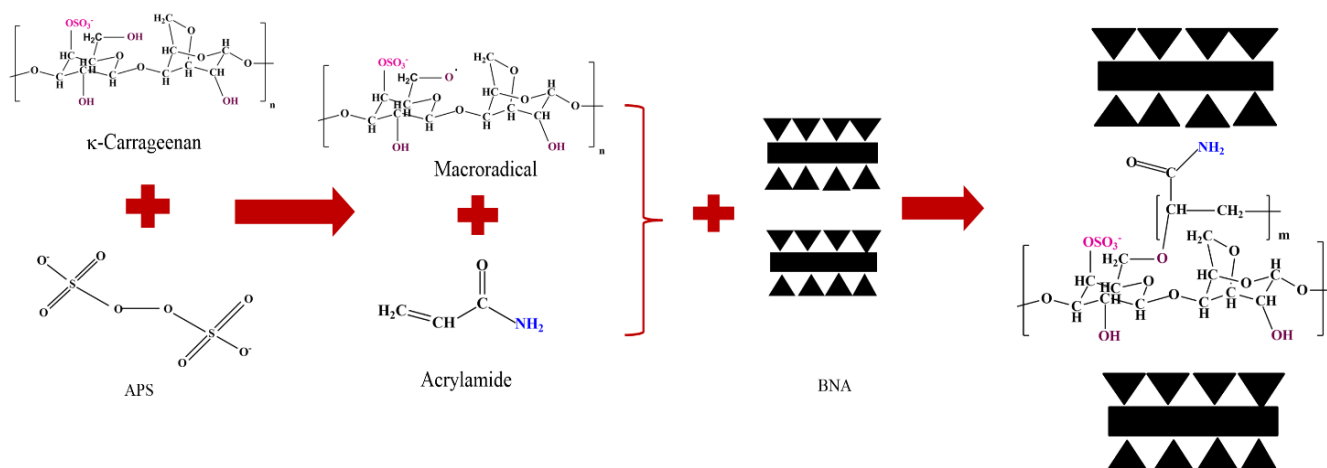
The ATR-FT-IR spectra of the samples were measured at 4  $\text{cm}^{-1}$  resolution and a mirror velocity of 0.6329  $\text{cm/s}$  in the 4000-500  $\text{cm}^{-1}$  region, on an Agilent Cary 600 Series FTIR Spectrometer equipped with DRIFT (Diffuse Reflectance Infra-red Fourier Transform) accessories. Five recordings were performed for each sample, and the evaluations were made based on the average spectrum.

#### 2.1.2. Thermogravimetric analysis measurements

Thermogravimetric analyses of the samples were performed by high-resolution TGA (TA Instruments Q Series Q600 SDT). 10 mg of finely ground sample was heated in an open platinum crucible with a heating rate of 10 °C  $\text{min}^{-1}$  and temperature from 50 to 800 °C under nitrogen atmosphere flow rate of 100  $\text{mL/min}$ .

#### 2.1.3. X-ray diffraction (XRD)

The measurements were performed on an X-ray diffractometer ULTIMA IV (Rigaku, Tokyo, Japan), using the  $\text{CuK}\alpha$  radiation ( $\lambda = 1.54 \text{ \AA}$ ) at 40 kV and 30 mA. All diffractograms were recorded in the 5-80  $2\theta$  degrees range at room temperature. A scan speed of 2°/min and a step size of 0.02° were considered to achieve measurements.



Scheme 1. BNA/κ-C/AM composite structure

### 3. Results and discussion

The composite was prepared by graft copolymerization of acrylamide onto κ-C in the presence of bentonite particles (Scheme 1).

Ammonium persulfate was used as an initiator. The persulfate is decomposed under heating and generates sulfate anion radicals that abstract hydrogen from OH groups of κ-C backbones. So, this persulfate-saccharide redox system results in active centers capable of radically initiating the polymerization of acrylamide, leading to a graft copolymer.

#### 3.1. FTIR analysis

FTIR spectroscopy was used for identification of the composites. Fig. 1(a) and Fig. 1(b) represent the spectra of κ-carrageenan and the different BNA/κ-C/AM composites, respectively.

The spectra of κ-carrageenan showed a broad absorption at 3440 cm<sup>-1</sup> and 2954 cm<sup>-1</sup> due to the stretching frequency of the O-H and C-H. The bands at 1256 cm<sup>-1</sup>, 922 cm<sup>-1</sup>, and 843 cm<sup>-1</sup> are attributed to the presence of sulfate groups and correspond to the sulfonic acid group, C-O stretching band, 3, 6-anhydro-D-galactose and glycosidic linkages of κ-C backbone, respectively [29].

On IR spectra of BNA/κ-C/AM composites, it was observed that the signal hydroxyl peak between 3450 cm<sup>-1</sup> and 3627 cm<sup>-1</sup> became stronger, which could be explained by the superposition of the stretching vibration of O-H groups in all materials.

The intensities of those FTIR characteristic peaks corresponding to κ-C in various BNA/κ-C/AM composites increased with the increase in κ-C mass.

The presence of PAM polymer in different composites is also confirmed by the apparition of a new band at 3193 cm<sup>-1</sup> corresponding to νN-H (sym). This band is more pronounced in C3 and C4 composites. The bands at 1607 and 1453 cm<sup>-1</sup> are ascribed to δN-H (amide II) and νC-N (amide III), respectively [30]. These findings confirmed that BNA/κ-C/AM composites structure was prepared successfully.

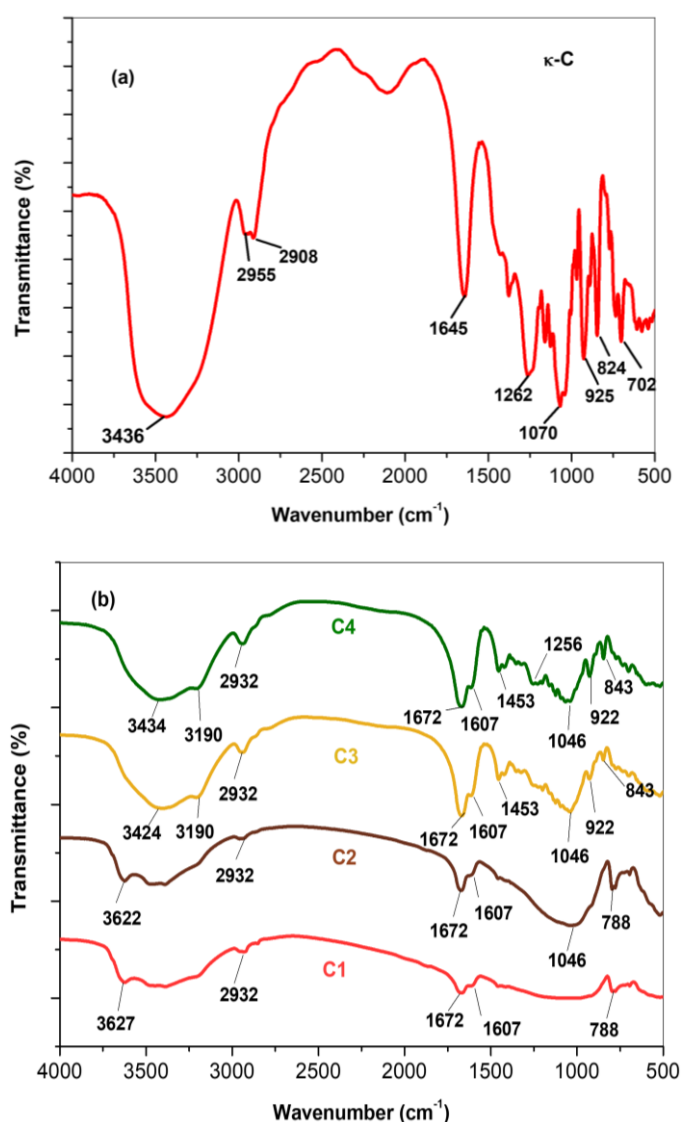


Figure 1. FTIR spectrum of κ-C (a), and BNA/κ-C/AM composites (b)

#### 3.2. Thermogravimetric analysis

The thermal stabilities of κ-carrageenan and its various composites were analyzed using thermogravimetric analysis (TGA), and the obtained resulting TGA curves are presented in Fig. 2.

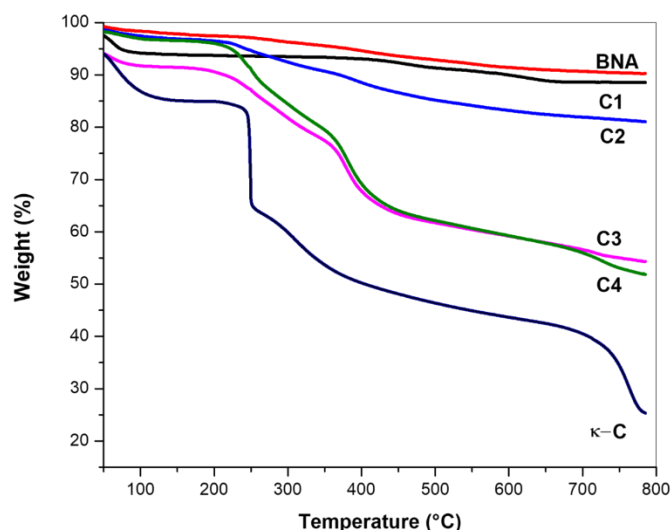


Figure 2. TGA curves of BNA,  $\kappa$ -C and BNA/ $\kappa$ -C/AM composites

It is seen from the Fig. 2 that the weight loss of pure  $\kappa$ -carrageenan occurred in three different stages. The first one, located in the temperature range of 45–150 °C, was due to the adsorbed water by  $\kappa$ -carrageenan. The decomposition of  $\kappa$ -carrageenan started at 203 °C. For  $\kappa$ -carrageenan, the second weight loss of 21.04% in the temperature range of 209–262 °C and the third weight loss of 38.4% in the temperature range of 262–785 °C were observed. The residual weight observed in pure  $\kappa$ -carrageenan is 25.35%. A similar thermal decomposition behavior was previously reported [31].

For BNA/ $\kappa$ -C/AM composites, the first degradation stage (50–150 °C) is also observed. This could be attributed to the loss of moisture content as hydrogen-bound water as well as the dehydration of BNA clay. With increasing temperature, both of the second and third degradation stages took place beyond 200 °C.

The second stage of decomposition occurred between 200 and 650 °C and corresponds to weight losses of 6.47, 6.64, 32.65, and 38.19% for C1 C2, C3, and C4 composites samples, respectively. These values are probably due to the degradations of  $\kappa$ -C and polyacrylamide. The random breaking chains of polysaccharide occur between 200 and 350 °C. In the range of temperature between 220 and 440 °C, the degradation is also due to both weight losses of  $\text{NH}_2$  of amide side groups in ammonia form and to chain breakdown of polyacrylamide [32].

On the other hand, the different BNA/ $\kappa$ -C/AM composites were found to be more thermally stable with increasing temperature than the pure polymer.

These observations could be related to the stability of BNA at higher temperatures since the dehydroxylation of the aluminosilicates within the BNA clay layers occurs at temperatures beyond 650 °C. As a result, BNA enhanced the stability of the developed composites and to the interaction between BNA particles and  $\kappa$ -C/AM mixture.

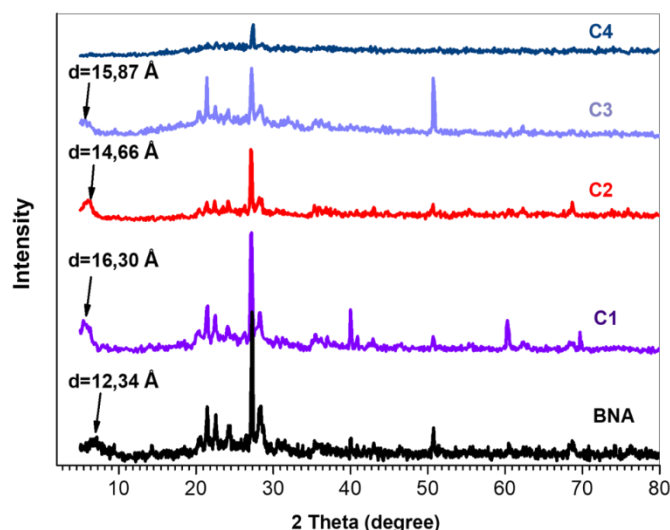


Figure 3. XRD patterns BNA and BNA/ $\kappa$ -C/AM composites

The obtained results are consistent with other studies that focused on studying the effect of clay encapsulation on the thermal behavior of beads prepared from other natural polysaccharides [33,34].

### 3.3. X-ray diffraction analysis

To reveal the state of the BNA sheets in the prepared composites, XRD measurements were carried out on the dried materials with various  $\kappa$ -C and AM contents. The XRD patterns of the different BNA/ $\kappa$ -C/AM composites with various weight ratios of  $\kappa$ -C and AM to BNA are shown in Fig. 3.

For  $\kappa$ -C, two signals were observed [35,36]: one at 4.5°, indicating the crystalline region, and a broad signal in the range of 12° to 25°, which reflects its semicrystalline nature.

The XRD of BNA contains a well-pronounced reflection at  $2\theta = 7.15^\circ$  (d spacing of 12.34Å), corresponding to the spacing between BNA sheets.

With increasing  $\kappa$ -C and AM content, the diffraction signals were shifted to lower values corresponding to basal spacings from 12.34Å to 16.3Å, 14.66Å and 15.87Å for C1, C2, and C3 composites, respectively. These results suggest the intercalation of polymer chains between BNA sheets [37,38].

The absence of the basal peak corresponding to montmorillonite phase in the case of C4 composite suggests a high dispersion of clay platelets, named exfoliation in the nanocomposite material.

## 4. Conclusion

A new composite material was prepared by graft copolymerization of AM onto  $\kappa$ -C in the presence of ammonium persulfate as the initiator and BNA particles.

A series of composites were prepared by varying  $\kappa$ -C and AM amounts. The obtained materials were



evaluated for their thermal stability, structural features, and interactions.

Infrared spectroscopy showed the presence of interactions between  $\kappa$ -C, AM, and BNA, especially via electrostatic interactions and/or hydrogen bonding.

The thermal stability of the resultant composites was significantly improved by the presence of BNA. The moisture adsorption of the prepared composites was reduced. This behavior is probably attributed to the interfacial interaction between the  $\kappa$ -C/AM mixture matrix and BNA.

X-ray diffraction revealed that the incorporation of BNA into the  $\kappa$ -C and AM enhances the formation of an intercalated nanocomposite structure in the case of C1, C2, and C3 samples, where the polymer chains were intercalated between the clay sheets. The formation of exfoliated nanocomposite structure in the case of the C4 sample is clear when  $\kappa$ -C and AM amounts were 1 g for each component.

## References

- [1] C. Erbil, D. Topuz, A. Gökçeören, B. Şenkal, Network parameters of poly(*N*-isopropylacrylamide)/montmorillonite hydrogels: effects of accelerator and clay content, *Polym Adv Technol*, 22, 2011, 1696-1704.
- [2] M. Ikeda, T. Yoshii, T. Matsui, T. Tanida, H. Komatsu, I. Hamachi, Montmorillonite-Supramolecular Hydrogel Hybrid for Fluorocolorimetric Sensing of Polyamines, *J Am Chem Soc*, 133, 2011, 1670-1673.
- [3] H. Kalaleh, M. Tally, Y. Atassi, Preparation of bentonite-g-poly(acrylate-co-acrylamide) superabsorbent polymer composite for agricultural applications: Optimization and characterization, *Polym Sci Ser B*, 57, 2015, 750-758.
- [4] W. Huang, J. Shen, N. Li, M. Ye, Study on a new polymer/graphene oxide/clay double network hydrogel with improved response rate and mechanical properties, *Polym Eng Sci*, 55, 2015, 1361-1366.
- [5] J. Du, P. Chen, A. Adalati, S. Xu, R. Wu, J. Wang, C. Zhang, Preparation and mechanical properties of a transparent ionic nanocomposite hydrogel, *J Polym Res*, 21, 2014, 1-6.
- [6] A. Rashidzadeh, A. Olad, D. Salari, A. Reyhanitabar, On the preparation and swelling properties of hydrogel nanocomposite based on Sodium alginate-g-Poly(acrylic acid-co acrylamide)/Clinoptilolite and its application as slow release fertilizer, *J Polym Res*, 21, 2014, 1-15.
- [7] A.A. Oun, J.W. Rhim, Carrageenan-based hydrogels and films: effect of ZnO and CuO nanoparticles on the physical, mechanical, and antimicrobial properties, *Food Hydrocoll*, 67, 2017, 45-53.
- [8] Z. Yao, F. Wang, Z. Gao, L. Jin, H. Wu, Characterization of a  $\kappa$ -Carrageenase from marine *Cellulophaga lytica* strain N5-2 and analysis of its degradation products, *Int J Mol Sci*, 14, 2013, 24592-24602.
- [9] G. Sun, T. Liang, W. Tan, L. Wang, Rheological behaviors and physical properties of plasticized hydrogel films developed from  $\kappa$ -carrageenan incorporating hydroxypropyl methylcellulose, *Food Hydrocoll*, 85, 2018, 61-68.
- [10] S. Lapwanit, T. Sooksimuang, T. Trakulsujaritchook, Adsorptive removal of cationic methylene blue dye by kappa-carrageenan/poly(glycidyl methacrylate) hydrogel beads: preparation and characterization, *J Environ Chem Eng*, 6, 2018, 6221-6230.
- [11] O. Levy-Ontman, C. Yanay, O. Paz-Tal, A. Wolfson, Iota-carrageenan as sustainable bio-adsorbent for the removal of europium ions from aqueous solutions, *Mater Today Commun*, 32, 2022, 104111.
- [12] B.I. Dogaru, B. Simionescu, M.C. Popescu, Synthesis and characterization of  $\kappa$ -carrageenan bio-nanocomposite films reinforced with bentonite nanoclay, *Int J Biologic Macromol*, 154, 2020, 9-17.
- [13] O. Goncharuk, O. Siryk, M. Frac, N. Guzenko, K. Samchenko, K. Terpilowski, K. Szewczuk-Karpisz, Synthesis, characterization and biocompatibility of hybrid hydrogels based on alginate,  $\kappa$ -carrageenan, and chitosan filled with montmorillonite clay, *Int J Biologic Macromol*, 278, 2024, 134703.
- [14] A. El Halah, J. Contreras, L. Rojas-Rojas, M. Rivas, M. Romero, F. López-Carrasquero, New superabsorbent hydrogels synthesized by copolymerization of acrylamide and *N*-2-hydroxyethyl acrylamide with itaconic acid or itaconates containing ethylene oxide units in the side chain, *J Polym Res*, 22, 2015, 1-10.
- [15] M. Ikeda, T. Yoshii, T. Matsui, T. Tanida, H. Komatsu, I. Hamachi, Rational Molecular Design of Stimulus-Responsive Supramolecular Hydrogels Based on Dipeptides, *J Am Chem Soc*, 133, 2011, 1670-1673.
- [16] J. Zhang, H. Chen, A. Wang, Study on superabsorbent composite-VII. Effects of organification of attapulgite on swelling behaviors of poly(acrylic acid-co-acrylamide)/sodium humate/organo-attapulgite composite, *Eur Polym J*, 42, 2006, 101-108.
- [17] X. Qi, M. Liu, Z. Chen, Study on swelling behavior of poly(sodium acrylate-co-2-acryloylamino-2-methyl-1-propanesulfonic acid)/attapulgite macroporous superabsorbent composite, *Polym Eng Sci*, 55, 2015, 681-687.
- [18] Q. Wang, W. Wang, J. Wu, A. Wang, Effect of Attapulgite Contents on Release Behaviors of a pH Sensitive Carboxymethyl Cellulose-g-Poly(acrylic acid)/ Attapulgite/Sodium Alginate Composite Hydrogel Bead Containing Diclofenac, *J Appl Polym Sci*, 124, 2012, 4424-4432.
- [19] A.K. Pradhan, P.K. Rana, P.K. Sahoo, Biodegradability and swelling capacity of kaolin based chitosan-g-PHEMA nanocomposite hydrogel, *Int J Biologic Macromol*, 74, 2015, 620-626.
- [20] X. Chen, J. Li, C. Mao, X. Jiao, Y. Liu, J. Gong, Y. Zhao, A Novel Superabsorbent Composite Based on Poly(Aspartic Acid) and Organo-Kaolin, *J Macromol Sci A*, 51, 2014, 799-804.
- [21] A. Pourjavadi, H. Ghasemzadeh, R. Soleyman, Synthesis, characterization, and swelling behavior of alginate-g-poly(sodium acrylate)/kaolin superabsorbent hydrogel composites, *Appl Polym Sci*, 105, 2007, 2631-2639.
- [22] Y.T. Zhang, L.H. Fan, T.T. Zhi, L. Zhang, H. Huang, H.L. Chen, Synthesis and characterization of poly(acrylic acid-co-acrylamide)/hydrotalcite nanocomposite hydrogels for carbonic anhydrase immobilization, *J Polym Sci A Polym Chem*, 47, 2009, 3232-3240.
- [23] W-F. Lee, Y-C. Chen, Effects of intercalated hydrotalcite on drug release behavior for poly(acrylic acid-co-*N*-isopropyl acrylamide)/intercalated hydrotalcite hydrogels, *Eur Polym J*, 42, 2006, 1634-1642.
- [24] N. Limparyoon, N. Seetapan, S. Kiatkamjornwong, Acrylamide/2-acrylamido-2-methylpropane sulfonic acid and associated sodium salt superabsorbent copolymer nanocomposites with mica as fire retardants, *Polym Degrad Stab*, 96, 2011, 1054-1063.
- [25] L.H. Fu, T.H. Cao, Z.W. Lei, H. Chen, Y.G. Shi, C. Xu, Biocompatible and biodegradable chitosan/sodium polyacrylate polyelectrolyte complex hydrogels with smart responsiveness, *Mater Des*, 94, 2016, 322-329.

- [26] H. Kalaleh, M. Tally, Y. Atassi, Preparation of bentonite-g-poly(acrylate-co-acrylamide) superabsorbent polymer composite for agricultural applications: Optimization and characterization, *Polym Sci Ser B*, 57, 2015, 750-758.
- [27] G.B. Marandi, M. Baharloui, M. Kurdtabar, Hydrogel with high laponite content as nanoclay: swelling and cationic dye adsorption properties, *Res Chem Intermed*, 41, 2015, 7043-7058.
- [28] S. Merad Boudia, K.I. Benabadji, B. Bouras, Graphene Oxide/Activated Clay/Gelatin Composites: Synthesis, Characterization and Properties, *Phys Chem Res*, 10, 2022, 143-150.
- [29] A.M. Salgueiro, A.L. Daniel-da-Silva, A.V. Girão, P.C. Pinheiro, T. Trindade, Unusual dye adsorption behavior of  $\kappa$ -carrageenan coated superparamagnetic nanoparticles, *Chemical Engineering Journal*, 229, 2013, 276-284.
- [30] R.M. Silverstein, G.C. Bassler, T.C. Morrill, *Spectrometric identification of organic compounds* (7. edition), 2013, New York, John Wiley & Sons.
- [31] O. Duman, T. Gürkan Polat, C. Özcan Diker, S. Tunç, Agar/ $\kappa$ -carrageenan composite hydrogel adsorbent for the removal of Methylene Blue from water, *International Journal of Biological Macromolecules*, 160, 2020, 823-835.
- [32] H. Ferfera-Harrar, H. Aiouaz, N. Dairi, Synthesis and Properties of Chitosan-Graft Polyacrylamide/Gelatin Superabsorbent Composites for Wastewater Purification World Academy of Science, Engineering and Technology International Journal of Chemical and Molecular Engineering, 9:7, 2015, 849-856.
- [33] N. Belhouchat, H. Zaghoulane-Boudiaf, C. Viseras, Removal of anionic and cationic dyes from aqueous solution with activated organo-bentonite/sodium alginate encapsulated beads, *Appl Clay Sci*, 35, 2017, 9-15.
- [34] A. Ely, M. Baudu, J.P. Basly, M.O. Kankou, Copper and nitrophenol pollutants removal by Na-montmorillonite/alginate microcapsules, *J Hazard Mater*, 171, 2009, 405-409.
- [35] A.M. Ili Balqis, M.A.R. Nor Khaizura, A.R. Russly, Z.A. Nur Hanani, Effects of plasticizers on the physicochemical properties of kappa-carrageenan films extracted from *Eucommia cottonii*, *Int J Biol Macromol*, 103, 2017, 721-732.
- [36] S. Shankara, J.P. Reddy, J.-W. Rhima, H.-Y. Kim, Preparation, characterization, and antimicrobial activity of chitin nanofibrils reinforced carrageenan nanocomposite films, *Carbohydr. Polym.* 117, 2015, 468-475.
- [37] M.J. Sanchis, M. Carsía, M. Culebras, C.M. Gómez, S. Rodriguez, F.G. Torres, Molecular dynamics of carrageenan composites reinforced with cloisite Na<sup>+</sup> montmorillonite nanoclay, *Carbohydr Polym*, 176, 2017, 117-126.
- [38] A. Pourjavadi, Z. Bassampour, H. Ghasemzadeh, M. Nazari, L. Zolghadr, S.H. Hosseini, Porous carrageenan-g-polyacrylamide/bentonite superabsorbent composites: swelling and dye adsorption behavior, *J Polym Res*, 23, 2016, 60.